Current Science
CS 6 (2), 6274-6287 (2026)
Received 16 March 2026 | **Accepted 04 April** 2026 | **Online Available 17 April** 2026
https://doi.org/10.52845/CS/2026-6-2-19

Current Science

Current Science

OPEN ACCESS

ISSN (O) 2795-8639

Original Article

Evolution of Pore Structure and Its Impact on Adsorption Performance of Coal Gangue before and After CO_2-Water-Rock Interaction

Deliang Fu[1], Kangning Zhang[2], Dan He[3], Xiang Gao[4], Bo Gao[5], Sida Zhang[6], Zixiang Wang[7]

[1,2,3]Key Laboratory of Coal Resources Exploration and Comprehensive Utilization, Ministry of Natural Resources (Shaanxi Coalfield Geology Group Co., Ltd.), Xi'an 710026, Shaanxi, China

[4,5,6]Shaanxi Tiandi Geology Co., Ltd., Xi'an 710021, Shaanxi, China

[7]Hubei Key Laboratory of Petroleum Geochemistry and Environment (Yangtze University)

***Corresponding Author: Deliang Fu**

Abstract: CO_2 geological sequestration using coal gangue backfilled in mined-out areas represents a crucial pathway for achieving synergistic pollution and carbon reduction. However, the dynamic modification mechanisms of complex CO_2-water-rock interactions on the pore structure of coal gangue, as well as their subsequent impacts on carbon sequestration potential, remain poorly understood. In this study, coal gangue with different initial occurrence states (crushed bulk rock and native dust) was investigated using a customized high-temperature and high-pressure dynamic reaction system to simulate the geological environment of mined-out areas (45 °C, 10 MPa). By integrating low-temperature N_2 and isothermal CO_2 adsorption characterizations—combined with BET, BJH, DFT, and D-R/D-A models—the cross-scale evolution characteristics of mesopores and micropores before and after the reaction were systematically and quantitatively analyzed.

The results indicate that: (1) The pore evolution pathways exhibit a strong initial-state dependency. Crushed bulk gangue generated a significant number of secondary micropores and broadened the mesopore throats, whereas the native gangue dust underwent severe physical clogging due to micropore collapse and precipitate migration. (2) The reconstruction of the micropore structure directly governs the maximum adsorption capacity. Quantitative analysis using the D-R model revealed that the reaction triggered a breakthrough 46.4% leap in the ultimate micropore volume (V_0) for the OXC-1 sample (reaching 7.382 cm^3/g), whereas the clogging effect led to an irreversible attenuation of V_0 for the FC-1 sample. (3) Macroscopic carbon sequestration performance is controlled by a cross-scale synergistic mechanism involving mesopore mass transfer and micropore storage; enhancing pore throat connectivity and increasing adsorption sites are essential prerequisites for improving adsorption performance. This study reveals the laws of pore reconstruction and evolution under gas-water-rock interactions in porous media, providing a theoretical foundation for site selection assessment and safety prediction for CO_2 geological sequestration in coal mine goafs.

Keywords : Coal gangue; CO_2 sequestration; Pore evolution; Water-rock interaction; Adsorption capacity

1. Introduction

Under the context of increasingly severe global climate change, Carbon Capture, Utilization, and Storage (CCUS) technologies have become a key pathway for achieving "dual carbon" goals [1-3]. Coal mining not only directly generates substantial greenhouse gas emissions but also produces massive amounts of coal gangue as solid waste [4-6]. Injecting CO_2 into abandoned coal

mine goafs and utilizing legacy or backfilled coal gangue for large-scale geological sequestration can effectively consume difficult-to-treat solid waste while achieving safe CO_2 storage [7-12], offering significant economic and environmental value. However, underground goafs represent a complex geological environment containing multiphase fluids. Injected high-pressure CO_2 dissolves in groundwater to form weakly acidic fluids, which then undergo long-term CO_2-water-rock geochemical and physical reactions with the coal gangue [13-20]. This process will inevitably etch, modify, or even destroy the internal skeleton of the coal gangue, thereby drastically altering its carbon sequestration capacity [13-18].

As a typical complex heterogeneous geological body, coal gangue possesses an extensively developed nanometer-scale pore network [31-36]. Studies have shown that the adsorption and storage of CO_2 in porous media are not independently completed by a single pore size but are synergistically controlled by pores of different scales [25, 31-33]. Among them, mesopores (2–50 nm) primarily serve as channels for long-distance diffusion of gas molecules, while micropores (< 2 nm) constitute the core adsorption sites for CO_2 due to strong surface potential energy overlap [21-26]. Recently, molecular simulation technologies have provided important means for revealing competitive adsorption mechanisms and micro-dynamic behaviors of CO_2 in coal matrices [27-29], demonstrating that CO_2 molecules have a significant adsorption advantage in multi-component gas competition due to their smaller kinetic diameter and higher critical parameters. However, most of these studies focus on pure coal or shale systems [21-29], and there remains a lack of systematic understanding regarding the cross-scale pore synergistic mechanism and dynamic evolution under CO_2-water-rock reactions for coal gangue—a complex heterogeneous solid waste.

Currently, scholars have conducted numerous studies on the pore evolution of pure coal or shale under water-rock interactions [13-20, 31-36], but discussions on the dynamic pore reconstruction mechanism for coal gangue as an artificial mixed solid waste are still seriously insufficient. In particular, coal gangue produced from different mechanical process stages (such as bulk rock versus long-term exposed native dust) differs significantly in initial physical structure, specific surface energy, and degree of weathering. Key scientific questions remain: will their pore networks expand through chemical dissolution or clog due to mineral detachment and precipitation when encountering acidic carbon-rich fluid intrusion[13-17].Furthermore, how does this structural evolution at micro and meso scales quantitatively map to macroscopic adsorption thermodynamic performance [21-26].These critical scientific issues have not yet been systematically revealed.

Based on this, this study selected three coal gangue samples with different process locations and initial occurrence states. Utilizing a customized high-temperature and high-pressure dynamic reaction system [13-15], the real environment of underground goafs (45 °C, 10 MPa) was highly simulated. By combining low-temperature N_2 and isothermal CO_2 adsorption experiments [31-36], and introducing macroscopic pore characterization methods (BET, BJH) alongside micropore filling theoretical models (DFT, Dubinin-Radushkevich, and Dubinin-Astakhov) [21-24], a comprehensive quantitative analysis of multi-scale pore characteristics before and after the reaction was conducted. This study aims to: elucidate the differentiated pore evolution paths of coal gangue with different initial states under the action of weakly acidic fluids; accurately quantify the impact of dynamic micropore reconstruction on the ultimate CO_2 adsorption potential; and reveal the control mechanism of the mesopore-micropore cross-scale synergistic network on macroscopic carbon sequestration performance. The results of this

study will not only enrich the theory of gas-water-rock interactions in complex geological bodies but also provide solid theoretical support for reservoir site selection and long-term safety prediction in practical coal mine goaf CO_2 sequestration engineering.

2 Materials and Methods

2.1 Sample Preparation and Experimental Apparatus

The raw coal gangue used in this experiment was sourced from a factory, specifically focusing on gangue from different mechanical process stages (belt, screw, and dust) as the research objects, designated as CSD, OXC, and FC series, respectively. Each series comprises four groups of samples, totaling 12 groups, where the CSD and OXC series initially existed in bulk form and the FC series was in powder form. To eliminate the interference of particle size differences on the internal pore structure and reaction kinetics tests, all raw samples were uniformly crushed and sieved to a specific particle size. Subsequently, an appropriate amount of deionized water was added to the reaction vessel containing the coal gangue powder and stirred thoroughly to prepare a uniform coal gangue slurry for the subsequent water-rock interaction experiments.

To simulate the actual geological environment of underground mined-out areas, this study utilized a customized high-temperature and high-pressure dynamic reaction system (Figure 1). The experimental system is primarily composed of two parts: a gas supply module and a high-pressure reaction module. High-purity carbon dioxide cylinders with a purity of 99.99% were used at the gas source end, where the gas passed through a stainless steel pressure regulator for precise pressure stabilization and flow control before being injected into the reaction system via a check valve, which effectively prevents the backflow of the high-pressure slurry.

The main reaction component is a stainless steel high-pressure autoclave equipped with a dynamic stirrer. A high-precision pressure gauge and a safety valve are installed at the top of the vessel to monitor the pressure of the top headspace in real-time and ensure experimental safety. The vessel is wrapped with a thermostatic heating device, capable of stably simulating the temperature and pressure conditions (up to 45°C and 10 MPa) of the underground mined-out area reservoir. During the experiment, the internal dynamic stirrer was activated to ensure full contact between the high-pressure CO_2 gas and the coal gangue slurry at the bottom under the set temperature and pressure conditions, thereby enhancing the mass transfer efficiency and mineralization processes at the gas-water-rock multiphase interface.

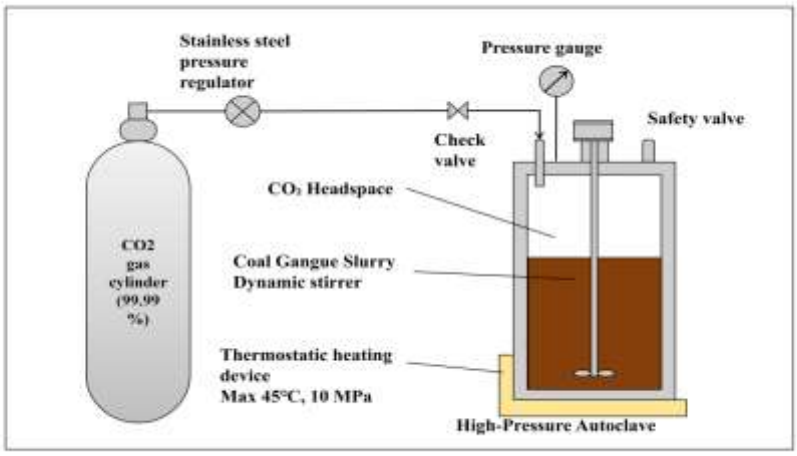

Figure 1|Customized high-temperature and high-pressure dynamic reaction system.

2.2 Pore Structure Testing

To comprehensively characterize the pore evolution features of coal gangue before and after the water-rock interaction, this study integrated low-temperature N_2 adsorption and isothermal CO_2 adsorption methods to jointly analyze the mesopore (2–50 nm) and micropore (< 2 nm) structures of the samples. Low-temperature N_2 adsorption experiments were conducted using high-purity nitrogen as the adsorbate to obtain isotherms by measuring adsorption and desorption volumes under various relative pressures; the specific surface area, mesopore volume, and pore size distribution were then calculated utilizing the BET equation and the BJH model. Given that CO_2 molecules possess a smaller molecular size and can access narrow channels more efficiently, isothermal CO_2 adsorption was specifically employed to characterize the micropore structure, with the Density Functional Theory (DFT) model used to resolve the specific surface area, pore volume, and concentrated distribution intervals of the micropores. The entire testing procedure and data processing strictly adhered to current national and industrial standards, including the *Static Adsorption Capacity Method for Determining Specific Surface and Pore Size Distribution of Rocks* (SY/T 6154-2019) and *Analysis of Micropores by Gas Adsorption* (GB/T 21650.3-2011).

2.3 Data Analysis Models

Because coal gangue develops a large number of nanometer-scale micropores, the adsorption behavior of CO_2 molecules within it no longer follows the conventional layer-by-layer surface coverage mechanism but instead aligns more closely with the micropore volume filling theory. To deeply analyze the micropore structure evolution and adsorption thermodynamic characteristics of coal gangue before and after the CO_2-water-rock interaction, this study introduced the Dubinin-Radushkevich (D-R) model and the Dubinin-Astakhov (D-A) model based on the Polanyi adsorption potential theory to mathematically resolve the isothermal CO_2 adsorption data.

The D-R model is an empirical model commonly used to describe the micropore filling adsorption mechanism on heterogeneous surfaces with a Gaussian energy distribution. This model is particularly suitable for physical adsorption processes within medium concentration ranges, and its linearized equation can be expressed as:

$$\ln V = \ln V_0 - D[\ln(P_0/P)]^2$$

where V represents the actual adsorbed volume of the gas at relative pressure P_0/P; V_0 represents the ultimate micropore volume, namely the maximum adsorption capacity when the micropores are completely filled ; and D is a constant related to the characteristic adsorption energy.

Considering that coal gangue, as a complex geological body, often exhibits extreme heterogeneity in its surface chemical properties and pore sizes, this study further introduced the D-A model. Compared to the D-R model, the D-A model provides higher flexibility and accuracy when dealing with microporous materials with structural heterogeneity. By introducing the heterogeneity index n, the D-A model can better adapt to materials with different pore structures. For highly heterogeneous coal-based solid waste microporous materials, this study set n=3, and its linear equation is expressed as:

$$\ln V = \ln V_0 - D'[\ln(P_0/P)]^3$$

where D' is also a constant related to the characteristic adsorption energy.

During the data processing, relationship scatter plots for the D-R and D-A models were respectively plotted and subjected to linear regression fitting. The accurate ultimate capacity was obtained from the intercept of the fitting line ($\ln V_0$), and the characteristic adsorption potential

energy between the gas and the adsorbent surface was further evaluated from the slope.

3 Results

3.1 Evolution of Mesopore Structure before and After the Reaction

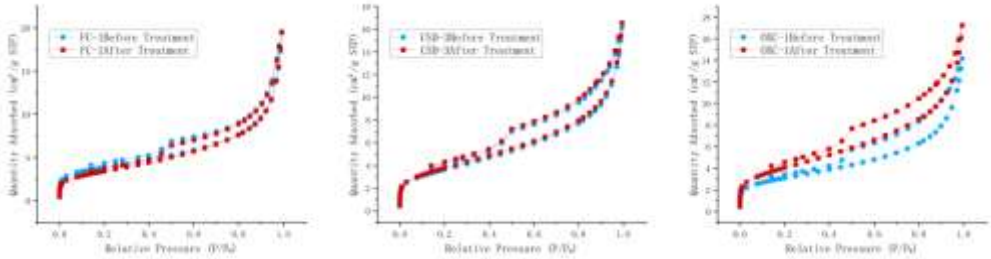

Figure 2|Low-temperature N_2 adsorption-desorption isotherms of coal gangue samples.

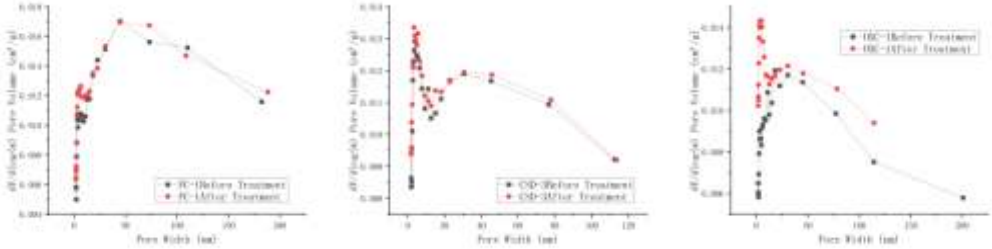

Figure 3|BJH pore size distribution curves of coal gangue samples.

The evolution characteristics of mesopore morphology and pore structure in coal gangue samples before and after the CO_2-water-rock interaction can be characterized by low-temperature N_2 adsorption-desorption isotherms (Figure 2) and the corresponding BJH pore size distribution curves (Figure 3). The test results demonstrate that the isotherms of all sample groups exhibit typical Type IV adsorption characteristics, with prominent H1-type hysteresis loops forming in the medium-to-high relative pressure region ($P/P_0 > 0.4$), indicating the extensive development of a porous network dominated by mesopores within the samples. Due to the heterogeneity of the initial pore structure and the varying sensitivity to the water-rock interaction, the three groups of samples exhibited three distinct mesopore evolution pathways after the reaction.

The OXC series samples exhibited the most significant pore expansion following the reaction. As seen in Figure 2, the OXC-1 sample before the reaction had a low total nitrogen adsorption volume and a flat curve, indicating that its primary mesopore network was limited in development. Following the gas-water-rock interaction, the adsorption branch showed a significant overall upward shift, and the hysteresis loop area expanded markedly. Combined with the corresponding pore size distribution curves in Figure 3, it is further revealed that OXC-1 experienced a sharp peak surge in the 2–50 nm mesopore range (particularly in the < 10 nm region) after the reaction. This phenomenon suggests that such samples underwent intense pore structure reconstruction during the process, giving rise to a large number of secondary mesopores, thereby significantly increasing the internal pore volume of the material.

The CSD series represents a case where the primary pores had a certain foundation and were

moderately improved after the reaction. As shown in Figure 2, the isotherms for CSD-3 before and after the reaction nearly overlapped in the low-pressure region, but the hysteresis loop area expanded to some extent in the medium-to-high pressure region where capillary condensation occurs. Its pore size distribution curve (Figure 3) maintained high consistency in morphology before and after the reaction, but the peak in the 2–20 nm range exhibited a mild overall elevation. This evolution pattern indicates that the water-rock interaction did not fundamentally alter the original pore skeleton but instead selectively widened the primary mesopore throats, thereby enhancing the connectivity and mass transfer capability of the pore network.

In contrast, the FC series samples demonstrated strong pore structure stability alongside localized attenuation characteristics. Their adsorption-desorption isotherms before and after the reaction almost completely overlapped, and the total nitrogen adsorption volume did not increase due to the water-rock interaction. More critically, the pore size distribution results in Figure 3 reveal that the curve for this sample in the large mesopore range of 10–50 nm was slightly lower than the pre-reaction stage. This phenomenon suggests that such samples are insensitive to the expansion and modification effects of the water-rock interaction; conversely, the peeling of fine particles or the generation of secondary precipitates accompanying the reaction may have caused physical clogging in some primary mesopore channels, leading to a slight decrease in local mesopore volume.

3.2 Evolution of Micropore Structure Before and After the Reaction

Coal gangue possesses an extensively developed network of nanometer-scale micropores, and its gas adsorption behavior no longer follows the conventional layer-by-layer surface coverage mechanism but aligns more closely with the micropore volume filling theory. In this study, the evolution of the micropore structure and the ultimate adsorption potential before and after the reaction were quantitatively resolved through isothermal CO_2 adsorption experiments (Figure 4) combined with the Dubinin-Radushkevich (D-R) and Dubinin-Astakhov (D-A) models (Figures 5 and 6).

Model fitting results indicate (Table 1) that the linear goodness of fit (R^2) for all representative samples under the D-R and D-A models ranged between 0.9854 and 1.0000, confirming that the micropore filling theory has extremely high applicability and accuracy in describing the ultra-low pressure adsorption behavior of such geological materials. Based on the physicochemical evolution characteristics of different samples, the reconstruction patterns of their micropore structures can be summarized into the following three pathways:

The OXC-1 sample exhibited the most significant micropore development features after the CO_2-water-rock interaction. As shown in Figure 4, its CO_2 adsorption capacity displayed a substantial overall increase as relative pressure increased. Quantitative data (Table 1) show that under the D-R model analysis, the ultimate micropore volume (V_0) of OXC-1 surged from 5.042 cm^3/g before the reaction to 7.382 cm^3/g, representing an increase of up to 46.4%. The evaluation results from the D-A model also confirmed this surging trend. These quantitative results intuitively indicate that the intense water-rock interaction not only greatly expanded the mesopore network of such samples but also induced the generation of a vast amount of secondary micropores at the microscopic scale, providing significant potential adsorption space.

The micropore evolution of the CSD-3 sample displayed a trend of steady expansion. Its CO_2 adsorption isotherm showed a moderate and continuous lift after the reaction (Figure 4). Through D-R model fitting calculations (Table 1), its micropore volume (V_0) grew steadily from

4.775 cm³/g to 6.924 cm³/g. The significant enhancement of this parameter suggests that the mild dissolution during the reaction effectively cleared fillings from some native micropore throats or converted partial closed/semi-closed micropores into effective interconnected pores, thereby steadily improving the ultimate micropore filling capacity of the material.

In stark contrast to the previous two groups, the micropore network of the FC-1 sample experienced capacity attenuation after the reaction. Observations of its isothermal adsorption curve show that the CO_2 adsorption capacity after the reaction was generally lower than the pre-reaction level (Figure 4). Mathematical resolution further quantified this attenuation (Table 1): its D-R ultimate micropore volume (V_0) decreased from an initial high baseline value of 7.949 cm³/g to 6.615 cm³/g. This characteristic indicates that the extremely rich native micropore structure in such samples failed to be effectively widened during the water-rock interaction; instead, microscopic structural compaction or physical filling by secondary precipitates induced by the reaction led to the loss and clogging of a large amount of micropore space, causing a slight irreversible decline in the overall adsorption capacity.

3.3 Changes in CO_2 Adsorption Capacity

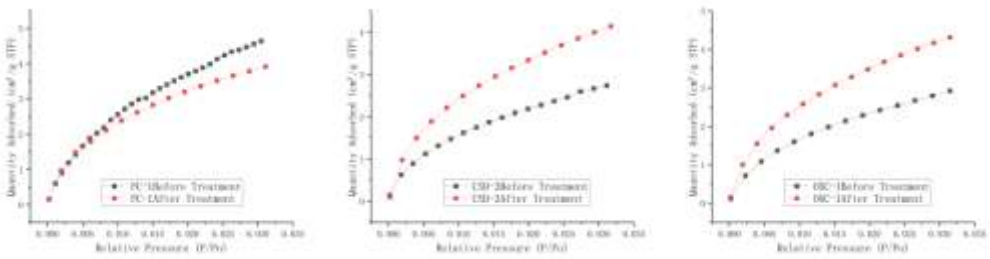

Figure 4|Isothermal CO_2 adsorption curves of coal gangue samples.

Isothermal CO_2 adsorption curves are not only used to resolve micro-pore parameters, but their absolute adsorption capacity serves as the most direct indicator for evaluating the actual CO_2 sequestration potential of coal gangue. As shown in Figure 4, within the extremely low test pressure range ($P/P_0 < 0.035$), the CO_2 adsorption capacity of the three representative sample groups exhibits a typical non-linear growth trend with increasing relative pressure, and shows differentiated characteristics before and after the water-rock interaction that are highly consistent with the pore evolution patterns.

The OXC-1 sample demonstrated the most superior CO_2 adsorption gain after the reaction. Observation of the right sub-figure in Figure 4 reveals that the adsorption isotherm after the reaction (red line) is significantly higher than that before the reaction (black line) throughout the entire test pressure interval. At the maximum test relative pressure ($P/P_0 \approx 0.031$), the actual CO_2 adsorption capacity jumped from 2.92 cm³/g before the reaction to 4.31 cm³/g, representing an extremely significant increase. This surge in macroscopic adsorption capacity directly maps to the generation of a large number of secondary micro/mesopores induced by the water-rock interaction as described previously, providing extremely abundant effective adsorption sites for CO_2 molecules.

The CO_2 adsorption curve of the CSD-3 sample exhibited a moderate and stable upward trend after the reaction. In the middle sub-figure of Figure 4, the post-reaction curve is positioned entirely above the pre-reaction curve; at the maximum relative pressure point, the adsorption

capacity increased steadily from 2.73 cm^3/g before the reaction to 4.13 cm^3/g. This growth trend indicates that while these samples did not undergo subversive structural reconstruction during the reaction, the improvement in pore connectivity and the widening of some pore throats effectively reduced the mass transfer resistance for gas molecules, thereby substantially enhancing the overall carbon sequestration performance of the material.

In stark contrast to the former two, the CO_2 adsorption capacity of the FC-1 sample exhibited a phenomenon of decrease rather than increase after the reaction. In the left sub-figure of Figure 4, the adsorption curve after the reaction is generally positioned below the pre-reaction curve. At the same maximum relative pressure, the adsorption capacity decreased from 4.64 cm^3/g to 3.92 cm^3/g. This decline in intuitive data irrefutably confirms that such highly stable pore skeletons are prone to physical clogging induced by the peeling of fine particles under long-term fluid interaction, ultimately resulting in the irreversible loss of effective adsorption space.

4 Discussion

4.1 Mechanisms of Pore Structure Change

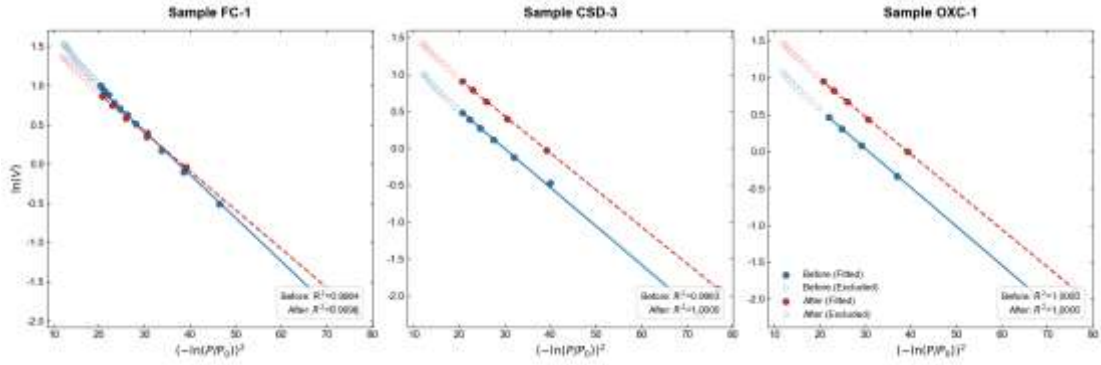

Figure 5|Dubinin-Radushkevich (D-R) model fitting for coal gangue samples.

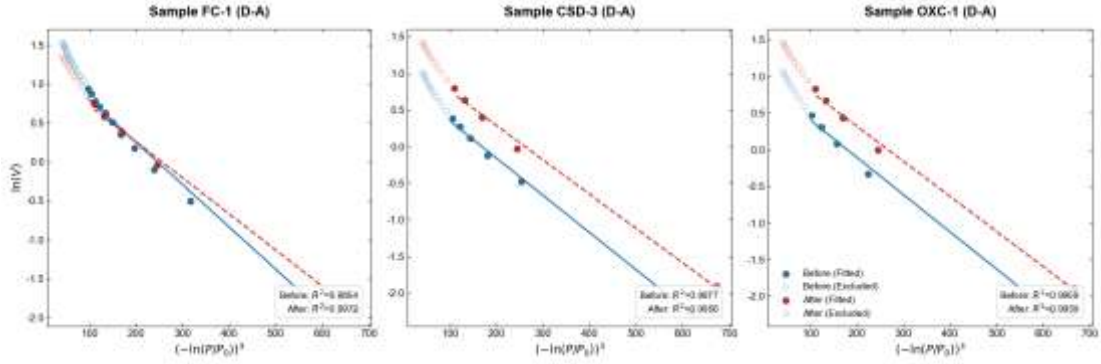

Figure 6|Dubinin-Astakhov (D-A) model fitting for coal gangue samples.

Table 1 Fitting parameters of D-R and D-A models for coal gangue samples

Sample	Treatment	D-R Model (n=2)				D-A Model (n=3)			
		ln V_0	**$V_0(cm^3/g)$**	***D***	**R^2**	**ln V_0**	**$V_0(cm^3/g)$**	***D'***	**R^2**
FC-1	Before	2.073	**7.949**	-0.05515	0.9984	1.342	**3.828**	-0.00544	0.9854
	After	1.889	**6.615**	-0.04945	0.9998	1.190	**3.288**	-0.00464	0.9972

CSD-3	Before	1.563	**4.775**	-0.05236	0.9993	0.856	**2.354**	-0.00507	0.9977
	After	1.935	**6.924**	-0.04998	1.0000	1.224	**3.402**	-0.00468	0.9956
OXC-1	Before	1.618	**5.042**	-0.05264	1.0000	0.911	**2.486**	-0.00508	0.9959
	After	1.999	**7.382**	-0.05092	1.0000	1.278	**3.590**	-0.00479	0.9959

Under the CO_2-water-rock interaction, the weakly acidic fluid formed by the dissolution of high-pressure CO_2 into water disrupts the stability of the original pore skeleton of the coal gangue. Based on the differences in the initial occurrence states, the modification pathways of the reactive fluid on the solid matrix are significantly different, which in turn exerts a decisive influence on the macroscopic CO_2 adsorption performance. The core evolution mechanisms can be summarized into the following three modes.

For the OXC series samples, which were crushed from bulk rock at the screw location, the interaction between the fluid and the gangue matrix is characterized by a strong secondary pore generation effect. Driven by the concentration gradient, the high-pressure acidic fluid intrudes into the dense matrix, producing an intense erosive effect on the new interfaces with high surface energy. This mineralization reaction leads to the localized dissolution of the solid skeleton, deriving a large number of secondary micropores and mesopores within the matrix that originally lacked porosity. The growth of secondary pores fundamentally reconstructs the adsorption network of the material. These newly generated nanometer-scale channels not only significantly increase the specific surface area but also provide dense effective adsorption sites for CO_2 molecules, directly contributing to the breakthrough growth in the ultimate micropore volume and actual adsorption capacity of these samples.

The CSD series also originates from bulk rock but possesses a certain initial pore network. In these samples, the acidic solution preferentially migrates along existing pore channels and micro-fractures. The effect of the solution on the pore walls is primarily manifested as mineralization and dissolution—that is, the mild dissolution and stripping of fragile substances adhering to narrow channels. This action does not significantly alter the overall topological structure of the pores but effectively widens the original water-rock interaction pathways and connects some previously isolated or semi-closed micropores. The clearing of pore throat channels effectively reduces the steric hindrance and mass transfer resistance for CO_2 molecule diffusion within the pore network. This significant improvement in connectivity allows gas molecules to enter the deep pore space more smoothly, thereby achieving a steady expansion of the overall adsorption capacity.

Since the FC series samples are inherently in a powder state, it is difficult for further significant mineralization-driven expansion to occur in these materials; conversely, the fragile pore structures of this series are highly susceptible to microscopic collapse, generating a large amount of detached fine precipitates. Due to the poor flow conditions in the deep micropores, these detached mineral precipitates are retained within narrow pore channels and ultimately become lodged at critical mesopore and micropore throats. This typical mineral migration and physical clogging effect lead to the physical isolation of a large amount of originally available native pores. Even if a substantial adsorption space exists within the material, CO_2 molecules are unable to enter due to channel occlusion, ultimately manifesting

macroscopically as the loss of effective adsorption space and an irreversible attenuation of absolute adsorption capacity.

4.2 Differential Impact of Initial Pore States

In complex porous geological media, the adsorption and sequestration of CO_2 are not independently completed by single-scale pores but are highly dependent on the synergistic matching of mesopore-micropore cross-scale pore structures. Among these, mesopores (2–50 nm) primarily serve as mass transfer channels for fluid migration, determining the gas diffusion process; meanwhile, micropores (< 2 nm), with their strong overlapping surface potential energy, constitute the primary adsorption and storage sites for CO_2 molecules, determining the total adsorption capacity. Combined with the previous characterization results, the differentiation in adsorption performance of coal gangue after the water-rock interaction is essentially the result of the mesopore-micropore synergistic mechanism being reconstructed to varying degrees.

The OXC series samples exhibited the most superior increase in CO_2 adsorption capacity after the reaction, rooted in the successful construction of a benign synergistic network of mass transfer and storage. Intense mineralization not only dissolved a large number of secondary micropores within the matrix, greatly expanding the gas adsorption space, but also generated numerous secondary fine mesopores with excellent connectivity to serve as mass transfer channels. This simultaneous cross-scale development allowed CO_2 molecules to rapidly penetrate the external gangue skeleton with extremely low diffusion resistance to reach newly generated deep micropore sites. The jump in ultimate micropore volume (V_0) resolved by the D-R model from 5.042 cm^3/g to 7.382 cm^3/g is the quantitative manifestation of this benign synergistic network in macroscopic adsorption thermodynamics.

For the CSD series samples, the improvement in adsorption performance is primarily attributed to the release of deep storage potential through the optimization of mass transfer channels. These samples inherently possess a certain number of native micropore adsorption sites, and the erosion of their pore throat surfaces by the water-rock interaction is equivalent to clearing the connecting pore throats. This significant improvement in connectivity converted native micropores, which were previously in a semi-closed state due to narrow throats, into effective adsorption sites; thus, steady expansion of the overall adsorption capacity was achieved solely through the reduction of mass transfer resistance.

The attenuation of adsorption capacity in the FC series reveals the negative effects of an imbalanced cross-scale synergistic mechanism from a kinetic perspective. This sample possessed an extremely high micropore baseline value before the reaction (V_0 reaching 7.949 cm^3/g), theoretically providing vast adsorption sites. However, mineral precipitation and physical clogging caused by the water-rock interaction primarily occurred at the mesopore throats, which serve as mass transfer hubs. Clogging at these critical nodes directly cut off the pathways for external gases to enter deep micropores, causing many originally connected micropores to become isolated. This phenomenon profoundly indicates that pure micropore volume, when detached from the effective connectivity of mesopore channels, cannot be converted into actual macroscopic adsorption capacity.

4.3 Engineering Applications for CO_2 Geological Sequestration

From the perspective of pore reconstruction and the synergistic evolution of mass transfer and storage, this study provides significant theoretical guidance and evaluation criteria for site selection in large-scale CO_2 geological sequestration projects within coal mine goafs. In actual underground mined-out environments, the initial

occurrence state of coal gangue exerts a decisive influence on its long-term CO_2 injectivity and sequestration security.

Based on the evolution patterns of the OXC and CSD series, crushed bulk coal gangue backfilled or left in goafs serves as a high-quality target reservoir for CO_2 sequestration. The injection of coal gangue slurry combined with CO_2 does not impair its seepage capability; rather, it continuously broadens fluid migration channels through intense secondary dissolution and pore throat erosion. This dynamic pore expansion effect effectively counteracts the closure stress of deep formations, maintaining a stable fluid injection rate over the long term. Concurrently, the massive quantity of secondary micropores generated by the reaction provides extensive space for capillary trapping and adsorption-based sequestration, ensuring the long-term safe retention of CO_2.

Conversely, the evolution characteristics of the FC series are unsuitable for such applications. Large amounts of coal gangue dust enriched at the bottom of goafs or near mining faces are highly susceptible to mineral precipitation and migration under long-term immersion and scouring by CO_2-rich fluids. These precipitates, migrating with the fluid, not only clog effective micropore adsorption spaces but also cause macroscopic permeability damage to the formation. This suggests that in practical engineering planning, the sequestration potential of dust-enriched zones must be cautiously evaluated to prevent the premature blockage of fluid injection channels.

In summary, utilizing coal gangue for CO_2 mineralization and adsorption-based sequestration is not a simple fluid injection process. Future engineering site selection and injection strategy designs must incorporate the initial occurrence state of the coal gangue and the dynamic pore evolution induced by water-rock interactions into the core analytical framework. This is essential to achieve the dual optimization of injection efficiency and sequestration capacity.

5 Conclusion

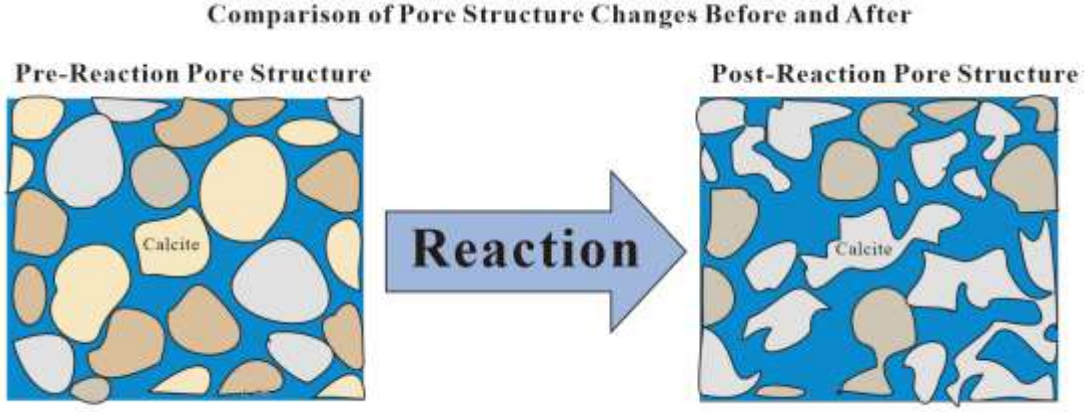

Figure 7|Comparison of Pore Structure Changes Before and After

This study systematically revealed the multi-scale pore evolution laws driven by CO_2-water-rock interactions and their control mechanisms over macroscopic adsorption performance by investigating coal gangue with different initial states under simulated real geological temperature and pressure environments. The primary conclusions are as follows:

1. **CO_2-water-rock interactions drive differentiated reconstruction of pore structures**. Crushed bulk gangue samples (OXC and CSD series) exhibited strong secondary

dissolution and pore throat erosion under the action of acidic fluids, effectively widening the pore throats for gas diffusion and generating a large number of secondary micropores. In contrast, the native dust-like samples (FC series) experienced severe physical clogging of critical mesopore and micropore throats due to micropore collapse and precipitate migration resulting from the reaction.

2. **The dynamic evolution of micropore structures directly determines the increase or decrease in CO_2 adsorption capacity**. Isothermal adsorption combined with D-R/D-A models accurately resolved the quantitative impact of pore reconstruction on ultimate adsorption potential. The mineralization reaction triggered a breakthrough 46.4% leap in the ultimate micropore volume (V_0) of the OXC-1 sample (reaching 7.382 cm^3/g), significantly enhancing the absolute adsorption capacity. Conversely, the pore throat clogging effect led to a decay in V_0 for the FC-1 sample (decreasing to 6.615 cm^3/g), resulting in a reduction of effective adsorption space.

3. **The mesopore-micropore cross-scale synergistic evolution mechanism dominates the final adsorption performance**. The improvement in the macroscopic CO_2 adsorption performance of coal gangue highly depends on the benign synergistic matching between mesopores and micropores. The improvement of pore throat connectivity and the derivation of micropore sites greatly reduced diffusion resistance and released storage potential. However, the clogging of mesopore mass transfer throats caused by the reaction cuts off the path for gas to enter deep micropores, causing them to degrade into ineffective isolated pores and fundamentally weakening the carbon sequestration efficiency of the material.

References

1. **Zhu L, et al.** (2025). Research on the Mechanical Activation Mechanism of Coal Gangue and Its CO_2 Mineralization Effect. Sustainability, 17(6),2364. **DOI:**10.3390/su17062364
2. **Zhu L, et al.** (2025). Investigation on the activation mechanisms of coal gangue and the corresponding CO_2 mineralization potential. Frontiers in Materials, 12,1567799.**DOI:**10.3389/ fmats.2025.1567799
3. **Huo W, et al.** (2023). Relationship between activity and specific surface area of acid-modified coal gangue for CO_2 capture. Fuel, 332,126045. **DOI:** 10.1016/j.fuel.2022.126045.
4. **Huo W, et al.** (2024). CO_2 capture capacity of gangue with acetic acid modification. Journal of Environmental Chemical Engineering, 12(1),109234. **DOI:**10.1016/j.jece.2023.109234
5. **Wu H, et al.** (2020). Mg-Cu-SiO_3 adsorbents from coal gangue for CO_2 capture. Chemical Engineering Journal, 389, 124450.**DOI:** 10.1016/j.cej.2020.124450
6. **Liu X, et al.** (2023). Effects of Supercritical CO_2 on the Pore Structure Complexity of High-Rank Coal with Water Participation. ACS Omega, 8(14), 12651-12665.**DOI:** 10.1021/acsomega.3c01486
7. **Meng J, Liao W, Zhang G.** (2021). Emerging CO_2-Mineralization Technologies for Co-Utilization of Industrial Solid Waste and Carbon Resources in China. Minerals, 11(3), 274.**DOI:** 10.3390/min11030274
8. **Huo B, Zhang J, Li M, Zhou N, Qiu X, Fang K, Wang X.** (2023). Effect of CO_2 Mineralization on the Composition of Alkali-Activated Backfill Material with Different Coal-Based Solid Wastes. Sustainability, 15(6), 4933.**DOI:** 10.3390/su15064933
9. **Lin X, et al.** (2024). Carbon dioxide sequestration by industrial wastes through mineral carbonation: Current status and perspectives. Journal of Cleaner Production,

434,140088.**DOI:** 10.1016/j.jclepro.2024.140088

10. **Wang L, et al.** (2025). Investigation of microstructural damage evolution in high-rank coal under supercritical CO_2 pulsating action. Geomechanics and Geophysics for Geo-Energy and Geo-Resources, 11(1), 1041.**DOI:** 10.1007/s40948-025-01041-x
11. **Liu X, et al.** (2023). Mechanical strength and porosity changes of bituminous coal induced by supercritical CO_2 interactions. Geoenergy Science and Engineering, 225, 211691.**DOI:** 10.1016/j.geoen.2023.211691
12. **Chen K, et al.** (2021). Influence of sequestered supercritical CO_2 treatment on the pore size distribution of coal across the rank range. Fuel, 306, 121708.**DOI:** 10.1016/j.fuel.2021.121708
13. **Liu X, et al.** (2023). Mechanical strength and porosity changes of bituminous coal induced by supercritical CO_2 interactions. Geoenergy Science and Engineering, 225, 211691.**DOI:** 10.1016/j.geoen.2023.211691
14. **Song Y, et al.** (2020). Changes in the microstructure of low-rank coal after supercritical CO_2 and water treatment. Fuel, 279,118493. **DOI:**10.1016/j.fuel.2020.118493
15. **Zhang H, et al.** (2024). Modeling of Supercritical CO_2 Adsorption for Low-Permeability Coal Seam of Huainan–Huaibei Coalfield, China. ACS Omega, 9(50), 50623-50635.**DOI:** 10.1021/acsomega.3c06599
16. **Liu X, et al.** (2023). Effects of Supercritical CO_2 on the Pore Structure Complexity of High-Rank Coal with Water Participation and the Implications for CO_2 ECBM. ACS Omega, 8(14),12651-12665.**DOI:** 10.1021/acsomega.3c01486
17. **Li H, et al.** (2025). Carbon sequestration in coal mine goafs using alkaline high-water materials solidified with supercritical CO_2. Clean Technologies and Environmental Policy, 27, 6587-6603.**DOI:** 10.1007/s10098-025-03187-9
18. **Cao G, et al.** (2024). Assessing the Performance of CO_2-Mineralized Underground Backfilling Materials through the Variation Characteristics of Infrared Radiation Temperature Index. Minerals, 14 (6), 566.**DOI:** 10.3390/min14060566
19. **Zardari ZH, Zhu H, Zheng X, Gan L, Liu S, Bhatti UA.** (2024). Comprehensive Review of CO_2 Adsorption on Shale Formations: Exploring Widely Adopted Isothermal Models and Calculation Techniques. ACS Omega, 9(50), 50623-50635.**DOI:** 10.1021/acsomega.4c04324
20. **Cai B, et al.** (2020). Potential impact of CO_2 injection into coal matrix in molecular terms. Chemical Engineering Journal, 401, 126071. **DOI:** 10.1016/j.cej.2020.126071
21. **Fan Z, et al.** (2023). Modeling of Supercritical CO_2 Adsorption for Low-Permeability Coal Seam of Huainan–Huaibei Coalfield, China. ACS Omega, 8(46), 44195-44211.**DOI:** 10.1021/acsomega.3c06599
22. **Xu C, et al.** (2023). Filling–adsorption mechanism and diffusive transport characteristics of N_2/CO_2 in coal: Experiment and molecular simulation. Energy, 282, 128428.**DOI:** 10.1016/j.energy.2023.128428
23. **Zhang J, et al.** (2024). Molecular modeling of CO_2 affecting competitive adsorption within anthracite coal. Scientific Reports, 14, 7286.**DOI:** 10.1038/s41598-024-58483-z
24. **Liu H, et al.** (2019). Supercritical-CO_2 Adsorption Quantification and Modeling for a Deep Coalbed Methane Reservoir in the Southern Qinshui Basin, China. ACS Omega, 4(7), 11685-11700.**DOI:** 10.1021/acsomega.9b01145
25. **Fang X, et al.** (2024). Integrated Multifractal Framework for Characterizing Full-Scale Pore Architecture of Deep Low-Rank Coal in Turpan-Hami Basin. Processes, 12(5), 946. **DOI:** 10.3390/pr12050946

26. **Wang D, et al.** (2024). Difference between coal and shale pore structural characters based on gas adsorption experiment and multifractal analysis. Fuel, 371, 132044.**DOI:** 10.1016/j.fuel.2024.132044
27. **Zhang Y, et al.** (2025). Characterization of the Multiscale Evolution of Coal Pore Structure Under Liquid CO2 Phase Change Fracturing. ACS Omega, 10(48), 46823-46835.**DOI:** 10.1021/acsomega.4c10256
28. **Zhang S, et al.** (2025). Fractal Characteristics of Multi-Scale Pore Structure of Coal Measure Shales in the Wuxiang Block, Qinshui Basin. Processes, 13(10), 3214.**DOI:** 10.3390/pr13103214
29. **Zhang S, et al.** (2025). Pore Structure and Fractal Characteristics of Coal Rocks Under Variable Moisture Content Increment Cycles Using LF-NMR Techniques. Water, 17(13), 1884.**DOI:** 10.3390/w17131884
30. **Wang J, et al.** (2021). Multi-fractal characteristics of pore structure for coal during the refined upgrading degassing temperatures. Journal of Petroleum Exploration and Production Technology, 11, 2931-2942.**DOI:** 10.1007/s13202-021-01226-x
31. **IEA** (2025). CCUS in Clean Energy Transitions: Regional Opportunities – China Policy Framework. International Energy Agency Report.**URL:** https://www.iea.org/reports/ccus-in-clean-energy-transitions
32. **Global CCS Institute** (2026). Policy Recommendations for Achieving CO_2 Geological Storage in China. Global CCS Institute Policy Report.**URL:** https://www.globalccsinstitute.com/resources/publications/
33. **Sang S, et al.** (2023). Research progress on technical basis of synergy between CO_2 geological storage potential and energy resources. Journal of China Coal Society, 48(7), 2700-2716.**DOI:** 10.13225/j.cnki.jccs.CN23.0316
34. **Zhang J, et al.** (2026). Potential evaluation and favorable zone optimization of CO_2 geological sequestration in deep coal reservoirs. Scientific Reports, 16, 42680.**DOI:** 10.1038/s41598-026-42680-z
35. **Zhang J, et al.** (2024). Molecular modeling of CO_2 affecting competitive adsorption within anthracite coal. Scientific Reports, 14, 7286.**DOI:** 10.1038/s41598-024-58483-z
36. **Liu Y, et al.** (2025). Molecular Dynamics Simulation of CO_2-ECBM Under Different Moisture Contents. Energies, 18(2), 239.**DOI:** 10.3390/en18020239